

Ligand-Controlled Mixed-Valence Copper Rectangular Grid-Type Coordination Polymers Based on Pyridylterpyridine

Lei Hou,^{†,§} Dan Li,^{*,†} Wen-Juan Shi,^{†,§} Ye-Gao Yin,[†] and Seik Weng Ng[‡]

Departments of Chemistry, Shantou University, Shantou, Guangdong 515063, P. R. China, and University of Malaya, 50603 Kuala Lumpur, Malaysia

Received April 11, 2005

Six mixed-valence Cu^ICu^{II} compounds containing 4'-(4-pyridyl)-2,2':6',2''-terpyridine (**L1**) or 4'-(2-pyridyl)-2,2':6',2''-terpyridine (**L2**) were prepared under the hydrothermal and ambient conditions, and their crystal structures were determined by single-crystal X-ray diffraction. Selection of CuCl₂·2H₂O or Cu(CH₃COO)₂·H₂O with the **L1** ligand and NH₄SCN, KI, or KBr under hydrothermal conditions afforded 1-dimensional mixed-valence Cu^ICu^{II} compounds [Cu₂(**L1**)(μ-1,1-SCN)(μ-Cl)Cl]_n (**1**), [Cu₂(**L1**)(μ-1)₂Cl]_n (**2**), [Cu₂(**L1**)(μ-Br)₂Br]_n (**3**), and [Cu₂(**L1**)(μ-1,3-SCN)₂(SCN)]_n (**4**), respectively. Compound **5**, prepared by layering with CuSCN and **L1**, is a 2-dimensional bilayer structure. In compounds **1–5**, the **L1** ligand and X (X = Cl, Br, I, SCN) linked between monovalent and divalent copper atoms resulting in the formation of mixed-valence rectangular grid-type M₄L₄ or M₆L₆ building blocks, which were further linked by X (X = Cl, Br, I, SCN) to form 1- or 2-dimensional polymers. The sizes of M₄L₄ units in **1–4** were fine-tuned by the sizes of X linkers. Reaction of Cu(CH₃COO)₂·H₂O with **L2** and NH₄SCN under hydrothermal conditions gave mixed-valence Cu^ICu^{II} compound [Cu₂(**L2**)(μ-1,3-SCN)₃]_n (**6**). Unlike those in **1–5**, the structure of **6** was constructed from thiocyanate groups and the pendant pyridine of **L2** left uncoordinated. The temperature-dependent magnetic susceptibility studies on compounds **1** and **4** showed the presence of mixed-valence electronic structure.

Introduction

Self-assembly processes involving carefully designed multidentate ligands and metal ions with appropriate stereo-electronic preferences provide effective means for the construction of different novel polymers such as molecular helicates, strings, grids, rings, and boxes.^{1–9} Grid-type compounds are of interest due to their predictable pore sizes,

selective inclusion of guest molecules, and interesting magnetic behaviors.^{3,9–13} Grids incorporating one type of metal center are easily built by selection of both metal centers and organic building blocks. Comparatively, the mixed-valence metal or regulable grid-type compounds are a synthetic challenge and scarcely reported;^{11,14} only few rectangular grid polymers have been reported.^{10,15–18}

In most cases, to design such grid-type complexes, the ligand requires an adequate number of binding sites and rigid

* To whom correspondence should be addressed. E-mail: dli@stu.edu.cn.

[†] Shantou University.

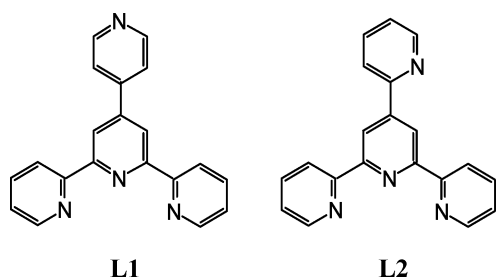
[§] Present address: Jiangxi Key Laboratory of Surface Engineering, Jiangxi Science and Technology Normal University, Jiangxi 330013, P. R. China.

[‡] University of Malaya.

- (1) Philp, D.; Stoddart, J. F. *Angew. Chem., Int. Ed. Engl.* **1996**, *35*, 1154.
- (2) Sailaja, S.; Rajasekharan, M. V. *Inorg. Chem.* **2000**, *39*, 4586.
- (3) Ruben, M.; Rojo, J.; Romero-Salguero, F. J.; Uppadine, L. H.; Lehn, J.-M. *Angew. Chem., Int. Ed.* **2004**, *43*, 3644.
- (4) (a) Hou, L.; Li, D. *Inorg. Chem. Commun.* **2005**, *8*, 128. (b) Hou, L.; Li, D. *Inorg. Chem. Commun.* **2005**, *8*, 190. (c) Li, D.; Shi, W.-J.; Hou, L. *Inorg. Chem.* **2005**, *44*, 3907.
- (5) Kitagawa, S.; Kitaura, R.; Noro, S.-i. *Angew. Chem., Int. Ed.* **2004**, *43*, 2334.
- (6) Ko, J. W.; Min, K. S.; Suh, M. P. *Inorg. Chem.* **2002**, *41*, 2151.
- (7) Halper, S. R.; Cohen, S. M. *Angew. Chem., Int. Ed.* **2004**, *43*, 2385.
- (8) Ruben, M.; Ziener, U.; Lehn, J.-M.; Ksenofontov, V.; Gütllich, P.; Vaughan, G. B. M. *Chem.—Eur. J.* **2005**, *11*, 94.
- (9) Biradha, K.; Fujita, M. *J. Chem. Soc., Dalton Trans.* **2000**, 3805.

- (10) Biradha, K.; Fujita, M. *Chem. Commun.* **2001**, 15.
- (11) Baxter, P. N. W.; Lehn, J.-M.; Kneisel, B. O.; Fenske, D. *Chem. Commun.* **1997**, 2231.
- (12) Uppadine, L. H.; Lehn, J.-M. *Angew. Chem., Int. Ed.* **2004**, *43*, 240.
- (13) Waldmann, O.; Hassmann, J.; Müller, P.; Hanan, G. S.; Volkmer, D.; Schubert, U. S.; Lehn, J.-M. *Phys. Rev. Lett.* **1997**, *78*, 3390.
- (14) Funeriu, D. P.; Lehn, J.-M.; Fromm, K. M.; Fenske, D. *Chem.—Eur. J.* **2000**, *6*, 2103.
- (15) Zheng, L.-M.; Fang, X.; Li, K.-H.; Song, H.-H.; Xin, X.-Q.; Fun, H.-K.; Chinnakali, K.; Razak, I. A. *J. Chem. Soc., Dalton Trans.* **1999**, 2311.
- (16) MacGillivray, L. R.; Groeneman, R. H.; Atwood, J. L. *J. Am. Chem. Soc.* **1998**, *120*, 2677.
- (17) Groeneman, R. H.; MacGillivray, L. R.; Atwood, J. L. *Chem. Commun.* **1998**, 2735.
- (18) Tong, M.-L.; Chen, X.-M.; Yu, X.-L.; Mak, T. C. W. *J. Chem. Soc., Dalton Trans.* **1998**, 5.

Chart 1



coordination motifs. The ligands 4'-(4-pyridyl)-2,2':6',2''-terpyridine (**L1**) and 4'-(2-pyridyl)-2,2':6',2''-terpyridine (**L2**) containing two independent metal-binding domains can coordinate to metals to yield macrocyclic oligomers¹⁹ or linear polymers²⁰ through coordination of the tridentate terpyridyl and the monodentate pyridyl (Chart 1). On the other hand, hydrothermal synthesis under high pressure and at low temperatures (100–200 °C) has been proved to be an effective method in preparing highly stable metal–organic coordination polymers.²¹ It has been reported that Cu^{II} ions can be reduced to Cu^I by 4,4'-bipyridine and pyridine derivatives under hydrothermal conditions, and many mixed-valence Cu^ICu^{II} species were prepared by this way.^{22–26} In contrast to those extensively studied ligands, substituted terpyridyl ligands have been essentially ignored. As far as we are aware, no mixed-valence Cu^ICu^{II}–terpyridyl compound has been reported. A rational consideration is that hydrothermal reactions of Cu^{II} with pyridylterpyridyl ligands may in-situ generate mixed-valence Cu^ICu^{II} compounds, in which monodentate pyridyl and the tridentate terpyridyl domains may satisfy the different preference of coordination geometry for Cu^I and Cu^{II}, respectively. The self-assembly of both monovalent and divalent copper ions with pyridylterpyridine ligands provides a new pathway to construct novel coordination polymers.

Herein, we report the preparation of several mixed-valence Cu^ICu^{II}–terpyridyl compounds based on 4'-(4-pyridyl)-2,2':6',2''-terpyridine (**L1**) and halogen or pseudohalogen X (Cl, Br, I, SCN) linkers, in which **L1** and X link two Cu^I and Cu^{II} atoms resulting in the formation of rectangular grid-type building blocks (Scheme 1). The sizes of the grids were fine-tuned by X linkers. For comparison, a mixed-valence Cu^ICu^{II} compound **6** of **L2** was also attained. The result shows that the ligand plays an important role in the construction of the rectangular grid-type building blocks.

(19) Sun, S.-S.; Lees, A. J. *Inorg. Chem.* **2001**, *40*, 3154.

(20) Hayami, S.; Hashiguchi, K.; Juhász, G.; Ohba, M.; Okawa, H.; Maeda, Y.; Kato, K.; Osaka, K.; Takata, M.; Inoue, K. *Inorg. Chem.* **2004**, *43*, 4124.

(21) Lu, J. Y. *Coord. Chem. Rev.* **2003**, *246*, 327.

(22) Lo, S. M.-F.; Chui, S. S.-Y.; Shek, L.-Y.; Lin, Z.; Zhang, X. X.; Wen, G.-H.; Williams, I. D. *J. Am. Chem. Soc.* **2000**, *122*, 6293.

(23) (a) Zhang, X.-M.; Tong, M.-L.; Chen, X.-M. *Angew. Chem., Int. Ed.* **2002**, *41*, 1029. (b) Zhang, X.-M.; Tong, M.-L.; Gong, M.-L.; Lee, H.-K.; Luo, L.; Li, K.-F.; Tong, Y.-X.; Chen, X.-M. *Chem.–Eur. J.* **2002**, *8*, 3187. (c) Huang, X.-C.; Zhang, J.-P.; Lin, Y.-Y.; Yu, X.-L.; Chen, X.-M. *Chem. Commun.* **2004**, 1100.

(24) Yaghi, O. M.; Li, H. *J. Am. Chem. Soc.* **1995**, *117*, 10401.

(25) Zhao, H.; Qu, Z.-R.; Ye, Q.; Wang, X.-S.; Zhang, J.; Xiong, R.-G.; You, X.-Z. *Inorg. Chem.* **2004**, *43*, 1813.

(26) Zheng, L.-M.; Yin, P.; Xin, X.-Q. *Inorg. Chem.* **2002**, *41*, 4084.

Experimental Section

All reagents were used as purchased without further purification. The ligand 4'-(4-pyridyl)-2,2':6',2''-terpyridine (**L1**) was prepared by a literature method, and 4'-(2-pyridyl)-2,2':6',2''-terpyridine (**L2**) by a modified procedure.^{27,28}

Physical Measurements. Infrared spectra were recorded with a Nicolet Avatar 360 FTIR spectrometer in the range of 4000–400 cm⁻¹, and samples were prepared as KBr pellets. Magnetic susceptibility data were collected at a field of 0.5 T on a Quantum Design magnetometer in the temperature range 2–300 K. The susceptibility data were corrected for the diamagnetic contributions as deduced by using Pascal's constant. Magnetization measurements were performed at 2 K and in the field range 0–7 T.

Preparations. 4'-(2-Pyridyl)-2,2':6',2''-terpyridine (**L2**). A solution of 2-acetylpyridine (3.63 g, 0.03 mol), 2-pyridinecarboxaldehyde (1.61 g, 0.015 mol), and NaOH (1.50 g) in water (30 cm³) and ethanol (30 cm³) was stirred for 15 h after which 100 cm³ water was added to give an orange oil. This oil was dissolved in a solution of NH₄OAc (10.00 g) in ethanol (80 cm³), and the mixture was refluxed for 8 h. The resulting solution was cooled, solvent reduced, and then treated with water (100 cm³) to give an orange precipitate which was collected by filtration. Recrystallization from acetone gave yellow crystals of **L2** (0.70 g, 15%), mp 232 °C. Anal. Calcd for C₂₀H₁₄N₄: C, 77.42; H, 4.52; N, 18.06. Found: C, 77.40; H, 4.55; N, 18.03%. IR (KBr, cm⁻¹): 3052 w, 3007 w, 1581 s, 1548 m, 1467 m, 1393 m, 1258 w, 1070 w, 993 m, 780 m.

[Cu₂(**L1**)(μ-1,1-SCN)(μ-Cl)Cl]_n (**1**). A mixture of CuCl₂·2H₂O (0.034 g, 0.2 mmol), ligand **L1** (0.062 g, 0.2 mmol), and NH₄SCN (0.030 g, 0.4 mmol) in the mole ratio 1:1:2 in ethanol (15 cm³) was sealed in a 20 cm³ Teflon-lined reactor, heated to 140 °C for 72 h, and then cooled to room temperature at a rate of 6 °C/h. X-ray-quality black crystals of compound **1** were obtained in ca. 55% yield. Anal. Calcd for C₂₁H₁₄Cu₂N₅Cl₂S: C, 44.53; H, 2.49; N, 12.36. Found: C, 44.50; H, 2.51; N, 12.33. IR (KBr, cm⁻¹): 3072 w, 2917 w, 2092 w, 1793 w, 1605 m, 1573 m, 1475 m, 1409 s, 1246 w, 1013 m, 792 m.

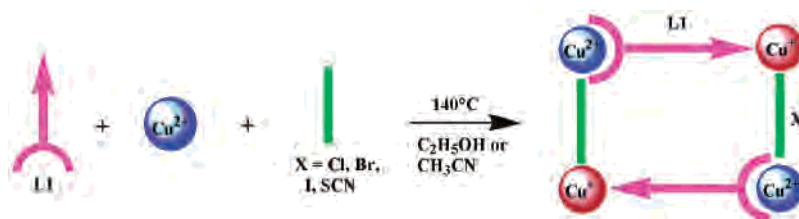
[Cu₂(**L1**)(μ-I)₂Cl]_n (**2**). It was prepared analogously to compound **1** by replacing NH₄SCN with KI in acetonitrile (15 cm³) in the same mole ratio. X-ray-quality black crystals of compound **2** were obtained in ca. 20% yield. Anal. Calcd for C₂₀H₁₄Cu₂N₄ClI₂: C, 33.05; H, 1.94; N, 7.71. Found: C, 33.08; H, 1.96; N, 7.68. IR (KBr, cm⁻¹): 3068 w, 2922 w, 1610 m, 1472 m, 1405 s, 1248 w, 1017 w, 875 w, 794 m.

[Cu₂(**L1**)(μ-Br)₂Br]_n (**3**). It was prepared analogously to compound **1** by replacing CuCl₂·2H₂O and NH₄SCN with Cu(CH₃COO)₂·H₂O and KBr in the same molar ratio. X-ray-quality black crystals of compound **3** were obtained in ca. 22% yield. Anal. Calcd for C₂₀H₁₄Cu₂N₄Br₃: C, 35.47; H, 2.08; N, 8.28. Found: C, 35.51; H, 2.05; N, 8.25. IR (KBr, cm⁻¹): 3062 w, 2920 w, 1604 m, 1476 m, 1403 s, 1245 w, 1017 w, 875 w, 790 m.

[Cu₂(**L1**)(μ-1,3-SCN)₂(SCN)]_n (**4**). It was prepared analogously to compound **1** by replacing CuCl₂·2H₂O with Cu(CH₃COO)₂·H₂O in the same mole ratio. X-ray-quality black crystals of compound **4** were obtained in ca. 52% yield. Anal. Calcd for C₂₃H₁₄Cu₂N₇S₃: C, 45.16; H, 2.31; N, 16.03. Found: C, 45.14; H, 2.34; N, 16.05. IR (KBr, cm⁻¹): 3050 w, 2921 w, 2092 s, 2063 m, 1646 m, 1540 m, 1405 m, 1046 m, 780 w.

(27) Kröhnke, F. *Synthesis* **1976**, 1.

(28) Constable, E. C.; Thompson, A. M. W. C. *J. Chem. Soc., Dalton Trans.* **1992**, 2947.

Scheme 1. M₄L₄ Rectangular Grid-Type Building Blocks in Compounds 1–4**Table 1.** Crystal Data and Structure Refinement Parameters for Compounds 1–6

param	1	2	3	4	5	6
formula	C ₂₁ H ₁₄ Cu ₂ N ₅ Cl ₂ S	C ₂₀ H ₁₄ Cu ₂ N ₄ ClI ₂	C ₂₀ H ₁₄ Cu ₂ N ₄ Br ₃	C ₂₃ H ₁₄ Cu ₂ N ₇ S ₃	C ₂₃ H ₁₄ Cu ₂ N ₇ S ₃	C ₂₃ H ₁₄ Cu ₂ N ₇ S ₃
<i>M_r</i>	566.41	726.68	677.16	611.67	611.67	611.67
<i>T</i> /K	293(2)	293(2)	293(2)	293(2)	293(2)	293(2)
wavelength (Å)	0.710 73	0.710 73	0.710 73	0.710 73	0.710 73	0.710 73
cryst system	monoclinic	triclinic	triclinic	monoclinic	triclinic	triclinic
space group	<i>P2₁/n</i>	<i>P1̄</i>	<i>P1̄</i>	<i>C2/c</i>	<i>P1̄</i>	<i>P1̄</i>
<i>a</i> (Å)	11.2411(8)	8.9683(5)	8.8681(18)	22.767(5)	8.2121(5)	7.2969(6)
<i>b</i> (Å)	14.4222(10)	9.3766(5)	9.2275(18)	13.547(3)	11.8356(8)	13.2198(10)
<i>c</i> (Å)	13.7402(10)	13.6302(8)	13.892(3)	15.010(3)	13.4445(9)	13.2833(10)
α (deg)		74.330(1)	73.87(3)		71.227(1)	111.543(1)
β (deg)	110.559(1)	78.684(1)	76.38(3)	92.180(4)	88.312(1)	96.854(1)
γ (deg)		84.784(1)	84.53(3)		73.112(1)	93.909(1)
<i>V</i> (Å ³)	2085.7(3)	1081.27(10)	1060.8(4)	4626.4(17)	1180.9(1)	1174.59(16)
<i>Z</i>	4	2	2	8	2	2
<i>D</i> _{calc} (g cm ⁻³)	1.804	2.232	2.120 1.756	1.720	1.729	
μ (mm ⁻¹)	2.416	4.960	7.669	2.138	2.094	2.106
reflens collcd	13 065	9440	7502	19365	10285	10202
unique reflens	4839	4906	4398	5419	5273	5230
<i>R</i> _{int}	0.0393	0.0173	0.0229	0.0537	0.019	0.0205
<i>GOF</i> on <i>F</i> ²	1.053	1.105	1.070	1.103	1.04	1.097
<i>R</i> 1, ^a <i>wR</i> 2 ^b [<i>I</i> > 2 σ (<i>I</i>)]	0.0521, 0.1087	0.0295, 0.0766	0.0593, 0.1757	0.0678, 0.1435	0.043, 0.110	0.0415, 0.1052
<i>R</i> 1, ^a <i>wR</i> 2 ^b (all data)	0.0785, 0.1198	0.0348, 0.0867	0.0746, 0.1882	0.1006, 0.1615	0.055, 0.122	0.0550, 0.1247

$$^a R1 = \sum |F_o| - |F_c| / \sum |F_o|. \quad ^b wR2 = [\sum w(F_o^2 - F_c^2)^2 / \sum w(F_o^2)^2]^{1/2}.$$

[Cu₂(L1)(μ -1,3-SCN)_{2.5}]_{*n*}·0.5*n*SCN (**5**). Ligand L1 (0.031 g, 0.1 mmol) was dissolved in 5 cm³ THF, and the solution was layered onto a saturated KSCN solution (5 cm³) containing CuSCN (0.012 g, 0.1 mmol). The solution was left for 2 weeks at room temperature. X-ray-quality black crystals of compound **5** were obtained in ca. 25% yield. Anal. Calcd for C₂₃H₁₄Cu₂N₇S₃: C, 45.16; H, 2.31; N, 16.03. Found: C, 45.17; H, 2.33; N, 16.07. IR (KBr, cm⁻¹): 3044 w, 2921 w, 2124 m, 2084 s, 1601 m, 1548 m, 1470 m, 1405 m, 1017 m, 788 w.

[Cu₂(L2)(μ -1,3-SCN)₃]_{*n*} (**6**). It was prepared analogously to compound **1** by replacing L1 with L2. X-ray-quality black crystals of compound **6** were obtained in ca. 30% yield. Anal. Calcd for C₂₃H₁₄Cu₂N₇S₃: C, 45.16; H, 2.31; N, 16.03. Found: C, 45.18; H, 2.29; N, 16.05. IR (KBr, cm⁻¹): 3056 w, 2921 w, 2088 s, 1614 m, 1556 w, 1475 m, 1413 m, 1021 w, 780 m.

Crystallography. Suitable crystals were mounted with glue at the end of a glass fiber. Diffraction data were collected at 293(2) K with a Bruker-AXS SMART CCD area detector diffractometer using ω rotation scans with a scan width of 0.3° and Mo K α radiation ($\lambda = 0.710 73$ Å). The crystal parameters and experimental details of the data collection are summarized in Table 1. Multiscan absorptions were applied.²⁹ The structure were solved by the direct methods and refined by full-matrix least-squares refinements based on *F*². All non-hydrogen atoms were refined with anisotropic thermal parameters, and all hydrogen atoms were included in calculated positions and refined with isotropic thermal parameters riding on those of the parent atoms. In compound **5**, two of the four thiocyanate groups are disordered over a center-of-inversion, and their atoms were refined with distance restraints of C–N

1.16±0.01, N–S 1.63±0.01, and N···S 2.79±0.02 Å. The temperature factors of the disordered atoms were restrained to be approximately isotropic. Structure solutions and refinements were performed with the SHELXL-97 package.³⁰ Selected bond lengths and angles are given in Table 2.

Results and Discussion

Crystal Structures. Single-crystal X-ray diffraction shows that each compound of **1–4** and **6** consists of a 1-D zigzag chain and **5** consists of a 2-D layer structure, respectively. The necessity to charge balance indicates that the metals have a mixed-valence Cu^ICu^{II} formulation. During the preparation of **1–4** and **6**, Cu^{II} ions were partly reduced by terpyridyl ligands. The possibility of reducing by halogen or pseudohalogen X cannot be ruled out. For **5**, Cu^I was partly oxidized in atmosphere. In **1–6**, the planar character of the tridentate motif of the terpyridyl ligands is critical in keeping the divalent copper ion at this site. In addition, from the preference of Cu^I bearing a tetrahedral coordination geometry and coordinating to sulfur atoms rather than nitrogen atoms,³¹ the valence state of the copper ions can also be expected.

[Cu₂(L1)(μ -1,1-SCN)(μ -Cl)Cl]_{*n*} (**1**). The asymmetric unit of **1** contains two crystallographically independent metal atoms in the crystal structure (Figure 1). The five-coordinated

(30) Sheldrick, G. M. *SHELXL-97, Program for the refinement of the crystal structures*; University of Göttingen: Göttingen, Germany, 1997.

(31) Bouwman, E.; Driessen, W. L.; Reedijk, J. *J. Chem. Soc., Dalton Trans.* **1988**, 1337.

(29) SADABS; Bruker AXS Inc.: Madison, WI, 2002.

Table 2. Selected Bond Lengths (Å) and Bond Angles (deg) for **1–6**^a

Complex 1			
Cu1–N1	2.051(3)	Cu2–S1	2.584(1)
Cu1–N2	1.951(3)	Cu2–S1 ^{#2}	2.259(1)
Cu1–N3	2.057(3)	Cu2–N4 ^{#1}	2.024(3)
Cu1–Cl1	2.237(1)	Cu2–Cl2	2.338(1)
Cu1–Cl2	2.486(1)		
N1–Cu1–N2	79.24(12)	N4 ^{#1} –Cu2–Cl2	100.57(10)
N2–Cu1–N3	78.51(12)	Cl1–Cu1–Cl2	98.62(4)
N1–Cu1–N3	156.62(12)	Cu1–Cl2–Cu 2	112.90(4)
Complex 2			
Cu1–N1	2.047(3)	Cu2–N4 ^{#2}	2.060(3)
Cu1–N2	1.946(3)	Cu2–I1	2.6112(6)
Cu1–N3	2.050(3)	Cu2–I2 ^{#1}	2.6059(6)
Cu1–Cl1	2.2450(10)	Cu2–I2	2.7278(6)
Cu1–I1	2.8660(6)		
N1–Cu1–N2	79.24(12)	Cl1–Cu1–I1	96.98(3)
N2–Cu1–N3	79.53(13)	N4 ^{#2} –Cu2–I 1	115.06(10)
N1–Cu1–N3	157.81(13)	Cu1–I1–Cu2	119.852(18)
Complex 3			
Cu1–N1	2.053(7)	Cu2–Br3 ^{#1}	2.5135(17)
Cu1–N2	1.947(6)	Cu2–Br3	2.6610(17)
Cu1–N3	2.063(7)	Cu2–N4 ^{#2}	2.045(6)
Cu1–Br1	2.3671(14)	Cu2–Br2	2.4855(16)
Cu1–Br2	2.7142(17)		
N1–Cu1–N27	9.6(3)	N4 ^{#2} –Cu2–Br2	118.0(2)
N2–Cu1–N3	79.0(3)	Br1–Cu1–Br2	97.28(5)
N1–Cu1–N3	157.2(3)	Cu1–Br2–Cu2	119.67(5)
Complex 4			
Cu1–N1	2.034(4)	Cu2–N4	2.052(4)
Cu1–N2	1.941(4)	Cu2–S1 ^{#1}	2.421(2)
Cu1–N3	2.034(4)	Cu2–S2	2.320(2)
Cu1–N5	1.938(4)	Cu2–S3	2.309(2)
Cu1–N6	2.133(5)		
N1–Cu1–N2	78.94(16)	N5–Cu1–N6	103.71(19)
N2–Cu1–N3	79.50(15)	N4–Cu2–S2	112.07(12)
N1–Cu1–N3	158.18(15)	S1 ^{#1} –Cu2–S 3	108.74(7)
Complex 5			
Cu1–N1	2.044(2)	Cu2–N4 ^{#1}	2.084(2)
Cu1–N2	1.942(2)	Cu2–S1	2.313(1)
Cu1–N3	2.055(2)	Cu2–S2 ^{#2}	2.357(1)
Cu1–N5	1.918(3)	Cu2–S3	2.214(2)
Cu1–N6	2.319(3)		
N1–Cu1–N2	79.8(1)	N5–Cu1–N6	95.3(1)
N2–Cu1–N3	79.3(1)	N4 ^{#1} –Cu2–S2 ^{#2}	111.5(1)
N1–Cu1–N3	158.4(1)	S1–Cu2–S3	107.8(1)
Complex 6			
Cu1–N1	2.056(3)	Cu2–N6	1.949(3)
Cu1–N2	1.928(2)	Cu2–N7	1.992(3)
Cu1–N3	2.041(3)	Cu2–S2	2.372(1)
Cu1–N5	1.924(3)	Cu2–S3	2.428(1)
Cu1–S1	2.655(1)		
N1–Cu1–N2	79.55(10)	N5–Cu1–S1	100.60(10)
N2–Cu1–N3	79.65(10)	N6–Cu2–N7	114.34(13)
N1–Cu1–N3	158.08(11)	S2–Cu2–S3	109.16(5)

^a Symmetry codes: (#1) $-x + 2, -y, -z + 1$, (#2) $-x + 1, -y, -z$ for **1**; (#1) $-x, -y, -z + 1$, (#2) $-x + 1, -y + 1, -z + 1$ for **2**; (#1) $-x + 1, -y + 2, -z$, (#2) $-x, -y + 1, -z$ for **3**; (#1) $-x + 1, -y + 2, -z$ for **4**; (#1) $x - 1, y - 1, z$, (#2) $x - 1, y, z$ for **5**.

divalent Cu2 has a distorted square pyramidal geometry [Cu–N 1.951(3)–2.057(3) Å, Cu–Cl 2.237(1)–2.486(1) Å] (see Table 2). Cl2 atom locates in the apical position and further bridges the other monovalent Cu1 atom [Cu–Cl 2.338(1) Å] with the Cu^I⋯Cu^{II} separation of 4.021 Å. The Cu2 atom rises from the N1–N2–N3–Cl1 basal plane to the apical Cl2 atom by 0.2768 Å. The values of the angles subtended by the terpyridyl unit [79.24(12) and 78.51(12)°] deviate from the ideal value of 90° being largely a conse-

quence of the geometric constraints imposed by **L1**.³² The monovalent Cu1 has a pseudotetrahedral mode. The sites are occupied by one pendant pyridine of **L1**, one chloride, and two thiocyanate groups [Cu–N 2.024(3) Å, Cu–S 2.259(1)–2.584(1) Å]. As expected, **L1** bridges Cu^I and Cu^{II} metal centers with the Cu2⋯Cu1B separation of 10.999 Å, leading to the formation of a mixed-valence tetrameric M₄L₄ rectangular grid-type building blocks.¹³ Compared with the common [2 × 2] grid-type structure,^{3,11} in **1**, the four metal centers define a pseudorectangle grid with a size ca. 11.0 × 4.0 Å and the angle Cu1⋯Cu2⋯Cu1B of 94.1°, the two **L1** ligands in a *transoid* arrangement to link Cu^I and Cu^{II}; thus, two Cu^I or Cu^{II} atoms are scattered oppositely at the corners. The pendant and central pyridines of **L1** are twisted with a dihedral angle 15.7°, and no intraunit face-to-face π – π interactions are observed. The adjacent grid-type M₄L₄ building blocks are linked between two Cu^I atoms by sulfur atom of the SCN group with an unusual μ -1,1-SCN coordination mode^{33,34} to form an infinite 1-D zigzag coordination polymer. The SCN group is almost linear [N–C–S 177.7(5)°]. The Cu^I⋯Cu^I distance of 2.643(1) Å is significantly shorter than those in complexes with μ -1,1-SCN bridges, indicating strong Cu^I⋯Cu^I interactions.³³ The chloride atoms are hydrogen bonded to aromatic carbon atoms from adjacent chains in the other *a* and *b* axes directions (C2⋯Cl1 3.562 Å, C2–H2⋯Cl1 161.7°; C20⋯Cl2 3.554 Å, C20–H20⋯Cl2 152.2°; see Table 3);³⁵ therefore, a 3-D network is constructed.

[Cu₂(L1)(μ -I)₂Cl]_n (**2**) and [Cu₂(L1)(μ -Br)₂Br]_n (**3**). Compounds **2** and **3** were prepared by replacing corresponding halogens under the same reaction condition for the preparation of **1**. X-ray diffraction shows compounds **2** and **3** have structural characters similar to those of **1**. The asymmetric unit of **2** and **3** (Figures 2 and 3) contain two crystallographically independent metal atoms in the crystal structures: a distorted square-pyramidal geometry divalent Cu2 and pseudotetrahedral monovalent Cu1 atom (see Table 2 for bond lengths and angles). As anticipated, mixed-valence tetrameric M₄L₄ rectangular units are observed. The two **L1** ligands in a *transoid* arrangement link Cu^I and Cu^{II}, with almost equivalent separations of 10.966 (for **2**) and 10.977 Å (for **3**), close to that in **1**. The I1 and Br2 atoms in **2** and **3** bridge Cu^I and Cu^{II} with the separations of 4.742 and 4.497 Å, respectively. Larger rectangular grids with the size ca. 11.0 × 4.7 Å and ca. 11.0 × 4.5 Å are formed with the Cu1⋯Cu2⋯Cu1B angles of 85.7 and 85.2° for **2** and **3**. As the atom radii of Cl, Br, and I increase, the short sides of the rectangular grids become longer. Within each tetrameric M₄L₄ unit in **2** and **3**, the pendant and central pyridines of **L1** are twisted with a dihedral angle 39.1 or 35.1°; the values larger than that in **1** may be attributed to the longer Cu^I⋯Cu^{II} separation supported by bigger halogen X (I, Br) atoms.

(32) Field, J. S.; Haines, R. J.; McMillin, D. R.; Summerton, G. C. *J. Chem. Soc., Dalton Trans.* **2002**, 1369.

(33) Kuang, S.-M.; Zhang, Z.-Z.; Wang, Q.-G.; Mak, T. C. W. *J. Chem. Soc., Dalton Trans.* **1997**, 4477.

(34) Goher, M. A. S.; Yang, Q.-C.; Mak, T. C. W. *Polyhedron* **2000**, *19*, 615.

(35) Steiner, T. *Angew. Chem., Int. Ed.* **2002**, *41*, 48.

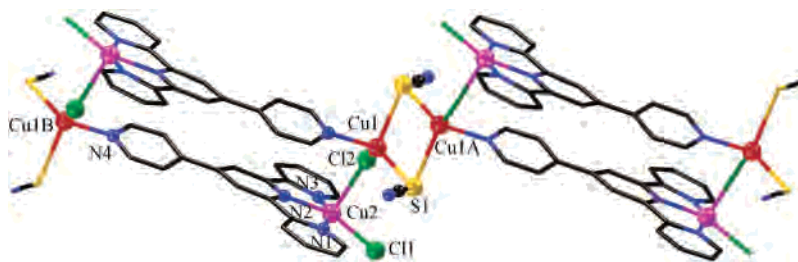


Figure 1. Perspective view of the structure **1** with partial atom numbering scheme. Hydrogen atoms are omitted for clarity. Symmetry codes: (A) $-x + 1, -y, -z + 1$; (B) $-x + 2, -y, -z + 1$.

Table 3. Hydrogen-Bonding Parameters in **1–4**^a and **6**^a

D–H···A	H···A (Å)	D···A (Å)	D–H···A (deg)
Complex 1			
C2–H2···Cl1 ^{#1}	2.668	3.562	161.7
C20–H20···Cl2 ^{#2}	2.705	3.554	152.2
Complex 2			
C2–H2···Cl1 ^{#1}	2.779	3.695	168.6
C20–H20···I2 ^{#2}	2.970	3.792	148.2
Complex 3			
C14–H14···Br1 ^{#1}	2.870	3.792	171.6
C20–H20···Br3 ^{#2}	2.808	3.666	154.0
Complex 4			
C13–H13···S3 ^{#1}	2.863	3.483	131.2
Complex 6			
C14–H14···S1 ^{#1}	2.755	3.500	140.9

^a Symmetry codes: (#1) $-x + 1/2, y - 1/2, -z + f$, (#2) $x + 1/2, -y + 1/2, z + 1/2$ for **1**; (#1) $x, y - 1, z - 1$, (#2) $-x + 1, -y + 2, -z + 1$ for **2**; (#1) $-x, -y + 2, -z + 1$, (#2) $x, y - 1, z$ for **3**; (#1) $x - 1/2, -y + 3/2, z - 1/2$ for **4**; (#1) $x - 1, y - 1, z$, (#2) $-x + 1, -y + 1, -z + 1$ for **5**.

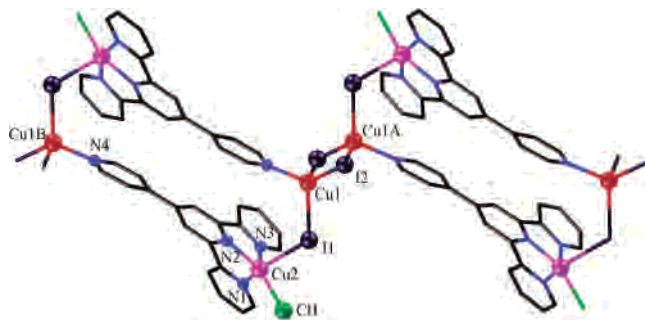


Figure 2. Perspective view of the structure **2** with partial atom numbering scheme. Hydrogen atoms are omitted for clarity. Symmetry codes: (A) $-x, -y, -z + 1$; (B) $-x + 1, -y + 1, -z + 1$.

As in **1**, the adjacent grid-type M_4L_4 units are linked between Cu^I centers by I or Br atoms in **2** and **3**, leading to the formation of an infinite 1-D zigzag coordination polymer. The $Cu^I \cdots Cu^I$ distance of 2.8380(12) and 2.812(3) Å for **2** and **3** are significantly longer than the value in **1**, in accord with the atom radii of I, Br, and S supported $Cu^I \cdots Cu^I$ separations in three compounds, respectively. In solid-state **2**, the Cl1 and I2 atoms are hydrogen bonded to carbons from adjacent chains in the other two directions [C2···Cl1 3.695 Å, C2–H2···Cl1 168.6°; C20···I1 3.792 Å, C20–H20···I1 148.2°, Table 3]³⁵ to construct a 3-D network. Similar network is also found in **3** with C14···Br1 of 3.792 Å and C20···Br3 of 3.666 Å (C14–H14···Br1 171.6°, C20–H20···Br3 154.0°, Table 3).^{35,36}

[$Cu_2(L1)(\mu-1,3-SCN)_2(SCN)_n$ (**4**). As shown in Figure 4, **L1** coordinates to divalent Cu^2 in the tridentate terpyridyl

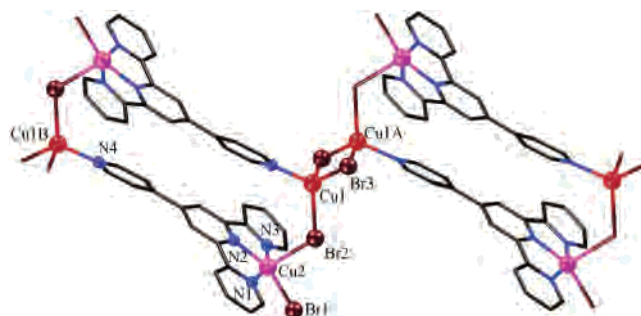


Figure 3. Perspective view of the structure **3** with partial atom numbering scheme. Hydrogen atoms are omitted for clarity. Symmetry codes: (A) $-x + 1, -y + 2, -z$; (B) $-x, -y + 1, -z$.

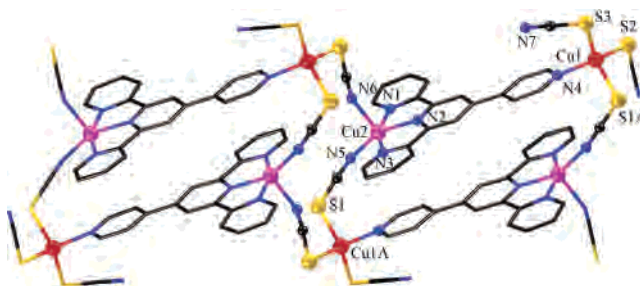
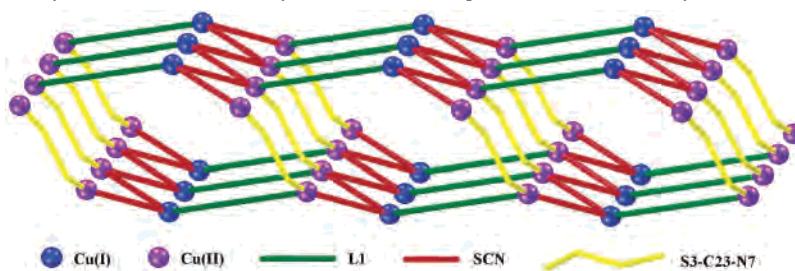


Figure 4. Perspective view of the structure **4** with partial atom numbering scheme. Hydrogen atoms are omitted for clarity. Symmetry codes: (A) $-x + 1, -y + 2, -z$.

side and to monovalent Cu^I in the monodentate pyridyl site with the $Cu^I \cdots Cu^I$ separations of 11.018 Å. The square-pyramidal geometry of Cu^I is completed by two N atoms of SCN groups [Cu–N 1.938(4)–2.133(5) Å, Table 2]. The Cu^I is surrounded by one N and three S atoms from three different SCN groups in a distorted tetrahedron environment. Cu^I and Cu^{II} are also linked by SCN groups in a $\mu-1,3-SCN$ mode, with “soft” S coordinating to Cu^I and “hard” N coordinating to Cu^{II} , to form a tetrameric M_4L_4 rectangular grid with a size ca. 11.0×5.5 Å ($Cu2 \cdots Cu1A$). The two **L1** ligands are in a *transoid* mode to link Cu^I and Cu^{II} ; thus, two Cu^I or Cu^{II} atoms are oppositely scattered at the corner with the angle $Cu1 \cdots Cu2 \cdots Cu1A$ of 126.0°. The longer short sides are consistent with the fact that SCN linkers are longer than halogen atoms in compounds **1–3**. The sizes of the tetrameric M_4L_4 rectangular unit are therefore fine-tuned through changing different halogen or pseudohalogen X. Within the tetrameric unit in **4**, two ligands possess an intramolecular $\pi-\pi$ interactions³⁷ (centroid-to-centroid 3.659

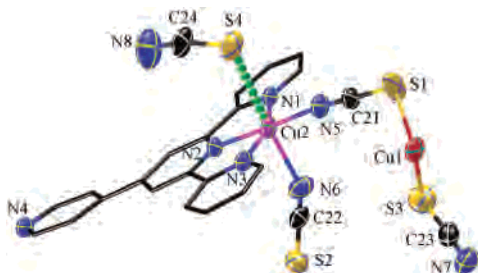
(36) Ouyang, X.-M.; Liu, D.-J.; Okamura, T.-a.; Bu, H.-W.; Sun, W.-Y.; Tang, W.-X.; Ueyama, N. *Dalton Trans.* **2003**, 1836.

(37) Janiak, C. *J. Chem. Soc., Dalton Trans.* **2000**, 3885.

Chart 2. 2-D Brick-Wall-like Bilayer Structure Connected by S3–C23–N7 Groups between Two Monolayers in **5**

Å), which may be responsible for less lean of 5.5° between pyridyl and terpyridyl motifs. Each tetrameric unit is doubly bridged by two μ -1,3-SCN groups to construct an infinite 1-D zigzag coordination polymer. The SCN groups are almost linear with the N–C–S bond angles in the range $176.0(5)$ – $178.8(6)^\circ$. Each Cu^{I} or Cu^{II} may be viewed as a connector between one tetrameric M_4L_4 unit and one 16-membered ring ($\text{Cu}^{\text{II}}\text{NCSCu}^{\text{I}}\text{NCSCu}^{\text{II}}\text{NCSCu}^{\text{I}}\text{SCN}$) with a grade of 98.2° (angle of $\text{Cu}^{\text{I}}\text{–Cu}^{\text{II}}\text{–Cu}^{\text{I}}$). Adjacent chains are closely packed with the shortest distance being an interchain $\text{S}\cdots\text{H}$ separation of 2.863 \AA ($\text{C13}\cdots\text{S3 } 3.483 \text{ \AA}$, $\text{C13–H13}\cdots\text{S3 } 131.2^\circ$, Table 3)³⁸ and are staggered each other.

[Cu₂(L1)(μ -1,3-SCN)_{2.5}]_n·0.5nSCN (5). Compound **5** was prepared by layering **L1** in THF onto saturated KSCN solution of CuSCN . Parts of monovalent copper were oxidized during the reaction. The asymmetric unit of **5** consists of two crystallographically independent copper atoms, one **L1**, and four thiocyanates (Figure 5). S3–C23–

**Figure 5.** Asymmetric unit of compound **5** showing the partial atom numbering scheme. The thermal ellipsoids are shown at the 50% probability level. Hydrogen atoms are omitted.

N7 and S4–C24–N8 groups are disordered over a center-of-inversion and were refined with occupancies of 0.5. The $\text{Cu2}\cdots\text{S4}$ contact is $2.977(5) \text{ \AA}$. In the solid state, compound **5** forms a 2-D brick-wall-like layer structure (Figure 6). As those in compounds **1–4**, **L1** in **5** links divalent Cu2 and monovalent Cu1 with the tridentate and monodentate pyridyl site, respectively. The coordination geometries of Cu1 and Cu2 in **5** are similar to those of **4** [$\text{Cu1–N4 } 2.084(2) \text{ \AA}$, $\text{Cu1–S } 2.214(2)$ – $2.357(1) \text{ \AA}$, $\text{Cu2–N } 1.918(3)$ – $2.319(3) \text{ \AA}$, Table 2]. The two SCN groups coordinated to divalent Cu2 adopt a μ -1,3-SCN mode to connect two monovalent Cu1 with the $\text{Cu}\cdots\text{Cu}$ separations 5.636 and 5.951 \AA , comparable with the corresponding separation in **4**. Notably, **L1** links two copper centers in a *cisoid* arrangement resulting

in a hexameric M_6L_6 rectangular grid-type unit with the lengths of long side of ca. 16.2 . The size of the unit is ca. $16.2 \times 6.0 \text{ \AA}$. The pyridyl and terpyridyl motifs are tilted by 3.1° . The hexameric unit are connected by **L1** and SCN groups along the two directions into a 2-D layer. In addition, S3–C23–N7 groups further link the other Cu^{I} centers into bilayer structure with the $\text{Cu}^{\text{I}}\cdots\text{Cu}^{\text{I}}$ separation of 5.910 \AA (Chart 2). In the solid state, no classic hydrogen bonds were found.

[Cu₂(L2)(μ -1,3-SCN)₃]_n (6). It seems that ligand **L1** with two discrete metal-binding domains plays a crucial role in the construction of rectangular grids. To examine the influence of the terpyridyl ligand on the structure, we replaced **L1** with **L2** and obtain compound **6** (Figure 7). The asymmetric unit of **6** is composed of two copper atoms, one **L2** ligand, and three SCN groups, which requires the copper atoms having a mixed-valence $\text{Cu}^{\text{I}}\text{Cu}^{\text{II}}$ formulation to balance charge. The divalent Cu2 geometry in **6** is similar those of **4** and **5**, except that the apical position is occupied by an S atom rather than the N atom of one SCN group with a longer Cu2–S1 distance of $2.655(1) \text{ \AA}$ comparing with a distance of $\text{Cu}^{\text{I}}\text{–S}$. The bond lengths and angles subtended by terpyridyl unit of **L2** are comparable with those of **1–5** (Table 2-6) [$\text{Cu–N } 1.928(2)$ – $2.056(3) \text{ \AA}$] (see Table 2). The $[\text{Cu}^{\text{II}}(\text{L2})(\text{SCN})_2]$ unit in **6** is attached to two Cu^{I} centers via two bridging SCN groups with a μ -1,3-SCN coordination mode, resulting in the formation of one 16-member $\text{Cu}^{\text{II}}\text{–NCSCu}^{\text{I}}\text{NCSCu}^{\text{II}}\text{NCSCu}^{\text{I}}\text{NCSCu}^{\text{I}}\text{NCSCu}^{\text{I}}\text{NCSCu}^{\text{II}}$ ring. The monovalent Cu1 has a distorted tetrahedron geometry with two N and two S atoms from four SCN groups [$\text{Cu–N } 1.949(3)$ – $1.992(3) \text{ \AA}$, $\text{Cu–S } 2.372(1)$ – $2.428(1) \text{ \AA}$]. Unlike in compounds **1–5**, the pendant pyridine of **L2** is uncoordinated and twisted about the central pyridines with a dihedral angle 12.7° . No grid-type building block was observed. The shortest distance between intermolecular uncoordinated pendant 2-pyridyl nitrogen and copper atom is 3.507 \AA . The $\text{Cu}^{\text{I}}\cdots\text{Cu}^{\text{II}}$ separations supported by SCN groups are 5.822 and 6.154 \AA . The SCN groups only coordinated to monovalent Cu1 adopt a μ -1,3-SCN coordination mode to bridge the other Cu^{I} atom with the $\text{Cu}^{\text{I}}\cdots\text{Cu}^{\text{I}}$ separation of 5.310 \AA shorter than 5.910 \AA in **5**, forming an infinite 1-D zigzag coordination polymer. The SCN groups, with the N–C–S bond angles in the range $177.8(3)$ – $178.9(3)^\circ$, are nearly linear similar with the values in **1** and **4**. In the solid state, π – π interactions³³ (centroid-to-centroid distance of 3.770 \AA) between pyridyl rings of the adjacent chains and interchain $\text{C–H}\cdots\text{S}$ hydrogen bonds ($\text{C}\cdots\text{S } 3.500 \text{ \AA}$, $\text{C–H}\cdots\text{S } 140.9^\circ$)³⁸

(38) Borrmann, H.; Persson, I.; Sandström, M.; Stålhandske, C. M. V. *J. Chem. Soc., Perkin Trans.* **2000**, 2, 393.

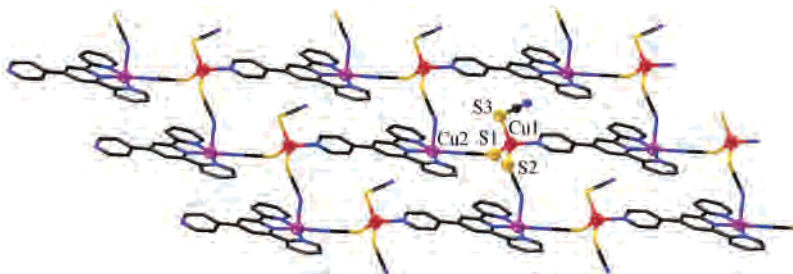


Figure 6. 2-Dimensional brick-wall-like layer structure of compound 5. Hydrogen atoms and uncoordinated SCN groups are omitted for clarity.

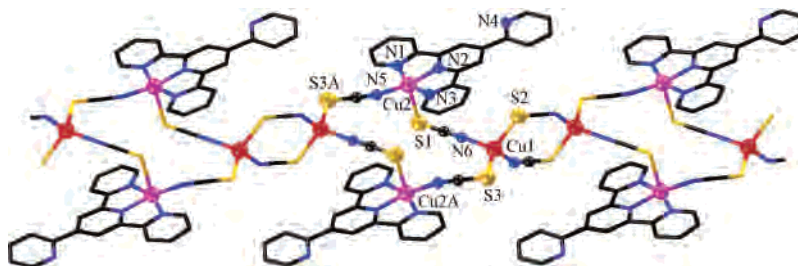


Figure 7. Perspective view of the structure 6 with partial atom numbering scheme. Hydrogen atoms are omitted for clarity. Symmetry codes: (A): $-x + 1, -y + 1, -z + 1$.

are responsible for the supramolecular 3-D structure of compound 6.

Infrared Spectra and Magnetic Properties. The infrared spectra for compounds 1–6 are similar showing characteristic bands of **L1** or **L2** in the $1650\text{--}1350\text{ cm}^{-1}$ range. In addition, paired bands were observed in the spectra of 4 and 5 at 2092, 2063 and 2124, 2084 cm^{-1} , respectively, assigned to $\nu_{\text{C}\equiv\text{N}}$ from SCN groups,³⁹ consistent with two different modes of SCN groups in 4 and 5. In contrast, a single peak was observed at 2092 cm^{-1} for 1 and 2088 cm^{-1} for 6, respectively.

Evidence for electronic structures of the mixed-valence complexes comes from the study of the temperature-dependent magnetic susceptibility on two typical complexes 1 and 4. The magnetic behaviors of compounds 1 and 4 are shown in Figure 8 in the form of μ_{eff} (effective magnetic moment/ Cu_2 unit) vs T . The magnetic behaviors for 1 and 4 obey the Curie–Weiss equation [$\chi_m = C/(T - \Theta)$], from which the Curie constant (C) and Weiss temperature (Θ) were obtained to be $0.417\text{ cm}^3\text{ K mol}^{-1}$, -17.480 K and $0.411\text{ cm}^3\text{ K mol}^{-1}$, -3.866 K (Figure 8). At room temperature, μ_{eff} values are 1.74 and $1.75\text{ }\mu_{\text{B}}/\text{Cu}_2$ unit for 1 and 4, respectively, which are close to the theoretical value $1.73\text{ }\mu_{\text{B}}$ expected for one isolated $S = 1/2$ spin, consistent with one unpaired electron/dimer. For 1, upon cooling, the μ_{eff} gradually decreases to $1.53\text{ }\mu_{\text{B}}$ at 20 K and then decreases sharply, reaching a value of $0.97\text{ }\mu_{\text{B}}$ at 2 K. Compared to 1, the μ_{eff} gradually decreases between 300 and 2 K from 1.75 to $1.66\text{ }\mu_{\text{B}}$. The continuous decreases of μ_{eff} for 1 and 4 upon cooling together with small Weiss temperature (Θ) indicate a weak intramolecular antiferromagnetic interaction^{23,40} of Cu^{II} ions through $\text{Cl}\text{--}\text{Cu}^{\text{I}}\text{--}\text{S}\text{--}\text{Cu}^{\text{I}}\text{--}\text{Cl}$ or $\text{L1}\text{--}\text{Cu}^{\text{I}}\text{--}\text{Cl}$ linkers in 1 and $\text{NCS}\text{--}\text{Cu}^{\text{I}}\text{--}\text{SCN}$ or $\text{L1}\text{--}\text{Cu}^{\text{I}}\text{--}\text{SCN}$ linkers in 4,⁴¹ and the interaction pathways caused by face-to-face $\pi\text{--}\pi$ interactions aside from the $\text{Cl}\text{--}\text{Cu}^{\text{I}}\text{--}\text{S}\text{--}\text{Cu}^{\text{I}}\text{--}\text{Cl}$ or $\text{NCS}\text{--}\text{Cu}^{\text{I}}\text{--}\text{SCN}$ also can be included. The sharp decrease of μ_{eff}

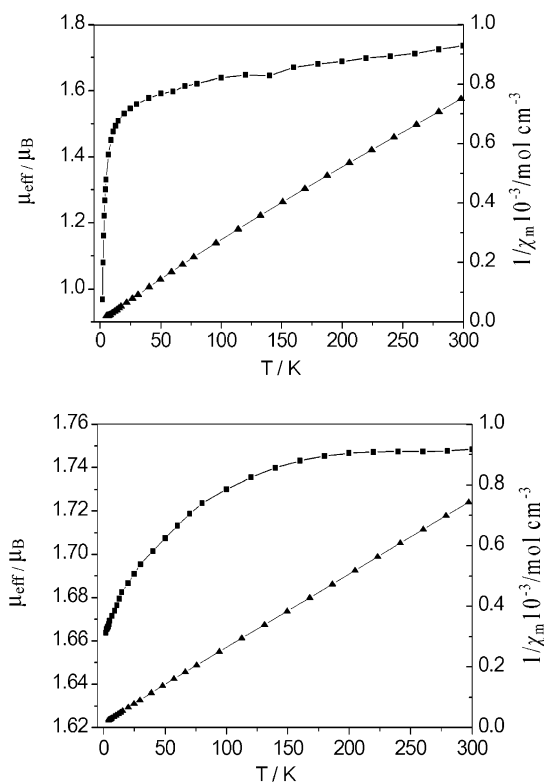


Figure 8. Temperature dependence of μ_{eff} (effective magnetic moment/ Cu_2 unit) (■) and $1/\chi_m$ (χ_m being the molar magnetic susceptibility/ Cu_2 unit) (▲) of compounds 1 (top) and 4 (bottom).

for 1 at low temperature exhibits stronger antiferromagnetic interactions⁴² than that in 4, which can be attributed to shorter

(39) Blake, A. J.; Brooks, N. R.; Champness, N. R.; Crew, M.; Hanton, L. R.; Hubberstey, P.; Parsons, S.; Schröder, M. *J. Chem. Soc., Dalton Trans.* **1999**, 2813.

(40) Zhang, X. X.; Chui, S. S.-Y.; Williams, I. D. *J. Appl. Phys.* **2000**, 87, 6007.

(41) Colacio, E.; Kivekäs, R.; Lloret, F.; Sunberg, M.; Suarez-Varela, J.; Bardají, M.; Laguna, A. *Inorg. Chem.* **2002**, 41, 5141.

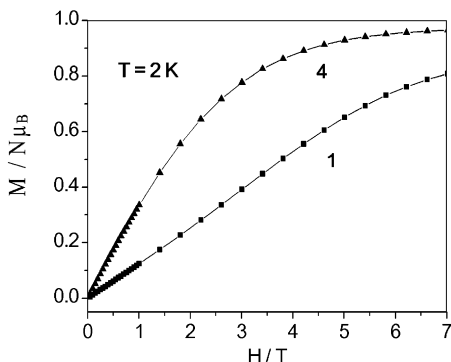


Figure 9. Magnetization isotherm plots at 2 K from 0 to 7 T for compounds **1** (■) and **4** (▲).

separations between two Cu^{II} ions in **1** compared to those in **4**, formed by different linkers.

To further study the electronic structures of **1** and **4**, the magnetization as a function of the applied magnetic field has been recorded at 2 K in range of 0–7 T for compounds **1** and **4** (Figure 9). Upon application of a magnetic field, the magnetization of **1** and **4** increases progressively. Saturation is almost reached at 7 T with a value of $0.965 N \mu_B$ for **4**, which is very near the theoretical value of $1 N \mu_B / \text{Cu}_2$ unit with $S = 1/2$. Compared to **4**, compound **1** is unsaturated at maximum field ($0.809 N \mu_B$ at 7 T), indicating weak intramolecular antiferromagnetic interactions,⁴³ which are in good agreement with stronger antiferromagnetic

interactions in **1** resulting from the shorter separations between two Cu^{II} atoms.

Conclusion

We have successfully performed the ligand-controlled aggregation of a series of structurally comparative mixed-valent Cu^ICu^{II}–terpyridyl compounds, in which rectangular grid-type M_4L_4 or M_6L_6 building blocks were further connected by halogen or pseudohalogen X (Cl, Br, I, SCN) linkers into 1-D chains or 2-D brick-wall-like bilayer structure. The sizes of grid units are fine-tuned by the sizes of the linkers. The studies on temperature-dependent magnetic susceptibility showed the presence of mixed-valence electronic structure. The successful design and synthesis of these compounds may provide a new route to the supramolecular self-assembly of mixed-valence grid-type compounds.

Acknowledgment. This study was financially supported by the National Natural Science Foundation of China (Grant Nos. 20271031 and 29901004) and the Natural Science Foundation of Guangdong Province (Grant No. 021240).

Supporting Information Available: Crystallographic data in CIF format. This material is available free of charge via the Internet at <http://pubs.acs.org>.

IC050558D

(42) Cano, J.; Munno, G. D.; Sanz, J. L.; Ruiz, R.; Faus, J.; Lloret, F.; Julve, M.; Caneschi, A. *J. Chem. Soc., Dalton Trans.* **1997**, 1915.

(43) Neels, A.; Stoeckli-Evans, H.; Escuer, A.; Vicente, R. *Inorg. Chem.* **1995**, *34*, 1946.